

# Relaxation behavior of polyurethane networks with different composition and crosslinking density



Martin Zajac<sup>a</sup>, Heike Kahl<sup>a,\*</sup>, Bernd Schade<sup>a</sup>, Thomas Rödel<sup>a</sup>, Madalena Dionisio<sup>b</sup>, Mario Beiner<sup>a,c</sup>

<sup>a</sup> Hochschule Merseburg, Fachbereich Ingenieur- und Naturwissenschaften, Eberhard-Leibnitz-Str. 2, 06217, Merseburg, Germany

<sup>b</sup> LAQV-REQUIMTE/CQFB, Departamento de Química, Faculdade de Ciências e Tecnologia, Universidade Nova de Lisboa, 2829-516, Caparica, Portugal

<sup>c</sup> Martin-Luther-Universität Halle-Wittenberg, Naturwissenschaftliche Fakultät II, Heinrich-Damerow-Str. 4, D-06120, Halle (Saale), Germany

## ARTICLE INFO

### Article history:

Received 7 September 2016

Received in revised form

9 January 2017

Accepted 16 January 2017

Available online 18 January 2017

### Keywords:

Polyurethanes

Dielectric spectroscopy

Relaxation behavior

Glass transition

## ABSTRACT

The relaxation behavior of a series of solvent free polyurethane model networks with variable cross-link density prepared based on different commercial diols and a diisocyanate containing component are studied by differential scanning calorimetry (DSC), dynamic-mechanical analysis (DMA) and dielectric relaxation spectroscopy (DRS). A systematic decrease of the calorimetric glass temperature  $T_g$  as well as of the softening temperatures  $T_{\alpha}^{DMA}$  and  $T_{\alpha}^{DRS}$  from relaxation methods is observed with increasing length of the diol sequences between neighbored diisocyanate units acting as cross-linker. This trend is explained based on an internal plasticization of the polymeric network by long, highly mobile diol units containing an increasing fraction of methylene sequences. Cold crystallization effects are only indicated for the longest diol sequence under investigation. This is understood as a consequence of a large fraction of methylene sequences in combination with weaker geometrical constraints. Two secondary relaxations,  $\beta$  and  $\gamma$ , are observed in the glassy state for all amorphous samples at low temperatures by dielectric spectroscopy indicating the existence of localized motions in the polyurethane networks. Below  $T_g$  these relaxation processes are practically unaffected by changes in the length of the diol units and the softening behavior of the polymeric model networks. Interrelations between secondary  $\beta$  relaxation and cooperative  $\alpha$  dynamics are indicated. An onset of the dielectric  $\alpha$  relaxation strength  $\Delta\epsilon_{\alpha}$  is observed for all amorphous polyurethane networks. A linear extrapolation of  $\Delta\epsilon_{\alpha}$  vs.  $1/T$  gives onset temperatures  $T_{on}$  which are in good agreement with  $\alpha\beta$  crossover temperatures  $T_{\alpha\beta}$  being the temperature where the difference between  $\alpha$  and  $\beta$  relaxation times  $\tau_{\alpha} - \tau_{\beta}$  approaches a minimum. This finding supports an onset of the cooperative  $\alpha$  motions in the  $\alpha\beta$  crossover region as reported in the previous literature for many other glass forming materials.

© 2017 Elsevier Ltd. All rights reserved.

## 1. Introduction

Polyurethane based materials are used in various fields of application because of their unique physical and chemical properties. Prominent examples are applications in arising technology fields such as coatings, adhesives, fibres, foams and thermoplastic elastomers [1–4]. Another interesting class of related materials are biocompatible composites based on polyurethane copolymers [5–7]. It is known that the properties of polyurethane based systems strongly depend on the polymolecularity of the soft segment

as well as on the overall chemical architecture of the components. Based on this phenomenological knowledge the properties of urethane-based materials can be systematically changed by variation of chemical composition, microstructure and molecular weight of the soft and hard segments [8,9]. By changing the functional groups proportion of the components  $r_H = [OH]/[NCO]$ , networks with variable topology were obtained [10,11]. In general, a complex three-dimensional network is formed which can be different regarding crosslinking density, functionality of the cross links (isocyanates) and the chain length of the binding molecules (diols). The network structure was investigated in different experimental and theoretical studies [12–16] and it was demonstrated that polyurethane networks possess commonly elastomer properties since they are used above their glass transition temperature  $T_g$ .

\* Corresponding author.

E-mail address: [heike.kahl@hs-merseburg.de](mailto:heike.kahl@hs-merseburg.de) (H. Kahl).

Many of the versatile properties of segmented polyurethanes making such materials interesting for industrial applications have been related to a nanophase separation tendency. Hence, several studies in the literature deal with the factors controlling nanophase separation and the development of experimental methods allowing to study nanophase separation in segmented polyurethanes [17–21]. Theoretical studies focusing on a statistical description of the network formation of polyurethane elastomers from soft segments and high polar hard segments are reported [22]. Dielectric studies on linear polyurethanes and polyurethane networks crosslinked using three-arm poly (propylene oxide) stars [23], molecular dynamics studies on linear and hyperbranched polyurethanes [24], as well as investigations of structure-property relations in polyurethanes with ionomers by thermoanalytical, spectroscopy or electrical methods [25–28] were performed. Structure and elasticity of model polyurethanes with well defined architecture were studied by Ilavsky and Dusek et al. [22,29] while the influence of the crosslink agent on the relaxations processes was systematically investigated by Opera [30,31].

In case of the commercially available polyurethane components Desmodur™ and Capa™, the NCO groups of Desmodur™ define the functionality of cross links, while different types of Capa™ can be used as binding agent between the polyisocyanates defining the mesh size of the network. Their length controls the distance between the cross links. The bridge length is in fact depending on molecular weight of the diol component since Capa™ contains only linear polyether diols. Hence, a high molecular weight of these diols causes a larger distance between two neighbored cross-links. It is known, that stiffness and glass transition temperature are usually systematically affected by the length of these bridges. This allows to prepare polyurethane model networks with systematically varied microstructure and network topology.

Aim of this work is to study polyurethane model networks prepared using different combinations of Desmodur™ and Capa™ by DSC and relaxation spectroscopy methods in order to learn more about the influence of network composition and topology on the overall relaxation behavior. Of special interest are (i) a better understanding of systematic changes in the softening behavior ( $T_g$ ,  $T_{\alpha}^{DMA}$ ,  $T_{\alpha}^{DRS}$ ) depending on the diol units used and (ii) interrelations between the segmental dynamics ( $\alpha$  relaxation) and localized motions seen as  $\beta$  and  $\gamma$  relaxations. Similarities to other polymeric systems containing short methylene sequences forming alkyl nanodomains will be used to explain details of the relaxations dynamics as well as the molecular origin of changes in the softening behavior. Analogies between polyurethanes model networks and many other glass forming systems regarding the relaxation behavior in the  $\alpha\beta$  crossover region are discussed.

## 2. Experimental

### 2.1. Materials and sample preparation

Polyurethane networks with variable cross-link density are prepared based on different commercial Capa™ (Perstorp Group) and Desmodur™ (BayerMaterials Science) components. Capa™ components being polyols with variable average lengths are used in combination with Desmodur™N3300 being a 1,6-hexamethylene diisocyanate-based system acting as crosslinking agent.

$\epsilon$ -caprolactone based systems of the Capa™2000 series exhibit a practically linear structure terminated with primary hydroxyl groups and have defined molecular weights (Scheme 1). The OH-values of the used Capa™2000 types were determined by titration. Their molecular weight correlates with the net bridge length of polymer networks if cross-linked with 1,6-hexamethylene diisocyanate. Capa™2043 is derived from 1,4-butanediol while all

other diols such as Capa™2054, Capa™2085, Capa™2125 and Capa™2205 are derived from diethylene glycole. Molecular weight  $M_w$  as well as average number of caprolacton units per diole  $n$  are systematically varied in the chosen diol series (Table 1) [32].

As cross linkers 1,6 hexamethylene diisocyanate (HDI) based mixtures from trimers, pentamers and heptamers are used. Main component in the used Desmodur™N3300 system (Scheme 1b) is the trimer of HDI [33]. The average functionality  $F$  specifying the mean number of free functional groups, in this case NCO-groups, per cross-linker molecule is  $F = 3.5$  for Desmodur™N3300.

The set specification of Capa™ and Desmodur™ was used for getting suitable mixtures with well defined molar ratios of the functional groups. In order to obtain a homogenous film, small amounts (0.2–0.5 wt%) of the additive BYK™332 (BYK Additives & Instruments) is added dropwise to the Capa™, followed by addition of Desmodur™ during stirring at 50 °C. This mixture was poured in preheated dishes of glass or Al-foil, which were heated within 30 min to 120 °C. After 24 h at 120 °C the preparation of the desire film was complete. The samples were than cooled down to 23 °C and investigated within two days.

### 2.2. Methods

Dielectric spectroscopy is used to study the frequency-temperature behavior of relaxation processes in the investigated polyurethane series. Dielectric measurements are performed with an impedance analyzer (Hewlett Packard HP 4282 A) covering the frequency range from 0.1 Hz to 1 MHz at sample temperatures ranging from –100 °C to 100 °C. Polyurethane films with a thickness of about 200  $\mu\text{m}$  kept between two gold-plated stainless-steel electrodes (diameter 20 mm) are used as sample capacitors. The samples are exposed to a temperature-controlled nitrogen gas stream. The sample temperature is measured with a PT100 sensor directly at the lower electrode and a Quatro Cryosystem from Novocontrol GmbH is used as temperature controller. The dielectric measurements are performed with the following steps: The sample (i) was annealed at –100 °C, (ii) ramped with a rate 10 K/min to 100 °C measuring four frequencies in order to find relevant relaxation processes, (iii) cooled down and annealed again at –100 °C, and (iv) heated in steps of  $T = 5$  K or  $T = 2$  K (depending on the temperature region) from –100 °C to 100 °C. In the latter case, the samples are annealed at least 15 min at each temperature in order to make sure that the control temperature was constant within an interval of  $\pm 0.02$  K.

Dynamic-mechanical measurements were carried out using a DMA242c dynamic mechanical analyzer (Netzsch GmbH). Oscillatory tests at a frequency of 1 Hz are performed in tensile mode with a strain amplitude of 70  $\mu\text{m}$  and a prestrain of 70  $\mu\text{m}$ . Stripes with a dimension of  $40 \times 5 \times 0,1$  mm<sup>3</sup> were cut from the prepared films. The dynamic modulus  $E^*$  was measured in the range from –120 °C to 50 °C, at a heating rate of 3 K min<sup>–1</sup> under nitrogen atmosphere. The variation of storage modulus ( $E'$ ), loss modulus ( $E''$ ) and loss tangent ( $\tan\delta = E''/E'$ ) as a function of temperature was recorded. Before measuring, the samples have been pretreated in an oven at 60 °C for at least 24 h to minimize the influence of humidity.

Differential scanning calorimetry (DSC) measurements were performed using a DSC200 (Netzsch GmbH). Measurements are carried out according a standard program. Samples with a mass of about 10 mg were (i) cooled from 25° to –120 °C at a rate of –10 K/min, (ii) held at –120 °C for 10 min, (iii) heated from –120 °C to 100 °C at a rate of +20 K/min, (iv) annealed at 100 °C for 10 min, (v) cooled to –120 °C with a rate of –10 K/min, (vi) held at that temperature for 10 min and finally (vii) reheated at a rate of +20 K/min to 100 °C. This second heating scan has been further evaluated. The glass temperature is determined based on a midpoint construction.

### 3. Results and discussion

DSC heating scans for polyurethane model networks with linear diol bridges of different lengths between neighbored diisocyanate units are presented in Fig. 1. All investigated samples show a well pronounced glass transition at temperatures between 0 °C and –40 °C.

The glass temperature  $T_g$  is systematically decreasing with increasing lengths of the diol sequences between neighbored diisocyanate units and increasing average fraction of methylene sequences in the diol units  $n$  (Table 1). This trend is interestingly comparable to that what is found with increasing length of the alkyl side groups in amorphous comb-like polymers like poly (n-alkyl methacrylates) [34,35], poly (n-alkyl acrylates) [36] or poly (di-n-alkyl itaconates) [37]. In that case, this effect has been interpreted as a consequence of an internal plasticization of polymer backbones by highly flexible CH<sub>2</sub> units in the side groups [38] accompanied by a nanophase separation of main and side chain parts [35]. Although the overall architecture of the polyurethane networks investigated here is quite different, the existence of highly mobile methylene sequences is a common aspect and may also explain the trend regarding the glass temperature  $T_g$  for the investigated polyurethane series. Peculiar behavior is only observed for the Capa™2205 based sample containing the longest diol sequences. This sample undergoes obviously cold crystallization above  $T_g = 39.9$  °C and melting at even higher temperatures. Crystallization and melting occur during heating at 0.9 °C and 23.4 °C, respectively. This finding can be also associated with the existence of long diol sequence between neighbored diisocyanate units having a strong crystallization tendency and feeling less constraints compared to systems with higher crosslink density. Heat of melting and heat of crystallization are 12.2 and 11.2 J/g for Capa™2205 based networks, respectively. Assuming that the methylene sequences do crystallize and that the heat of melting is about 3.4 kJ/mol per mole CH<sub>2</sub> unit, one can conclude that the diol sequences are only partly crystallizable. This might be reasonable considering length of the diol sequences and fraction of methylene units in Capa™2205 (Table 1 and Scheme 1).

Data for the elastic modulus,  $E' = E' + E''$ , measured at a frequency of 1 Hz by dynamic-mechanical analysis are presented in Fig. 2. The results confirm the trends seen in DSC heating scans. The dynamic glass transition ( $\alpha$  relaxation) shows a similar shift towards higher temperatures within the investigated polyurethane series. High  $\alpha$  relaxation temperatures  $T_{\alpha, 1\text{Hz}}^{\text{DMA}}$  are observed for Capa™2043 based systems with a small average number of alkyl carbons per diol sequence ( $n = 2.7$ ) while low  $T_{\alpha, 1\text{Hz}}^{\text{DMA}}$  values are

**Table 1**  
Sample characteristics.

	R	$M_w$ g/mol	$n^a$	$\nu^b$ mol/m <sup>3</sup>
Capa™2043	1,4 butanediol	400	2.7	1085
Capa™2054	diethylene glycol	550	3.9	898
Capa™2085	diethylene glycol	830	6.4	578
Capa™2125	diethylene glycol	1250	10.0	359
Capa™2205	diethylene glycol	2000	16.6	–

<sup>a</sup> Average number of carbons per diole sequence  $n = p + o$  (cf. Scheme 1a).

<sup>b</sup> Average crosslink density estimated based on a simple rubber elasticity model  $\nu = E_N^0/3RT$  with  $E_N^0$  being the elastic modulus in the rubber plateau range and  $R$  being the gas constant (cf. Fig. 2).

detected for the Capa™2205 containing sample with  $n = 16.6$ . If defined based on the maximum of the  $\alpha$  relaxation peak in the loss modulus  $E''$ , the relaxation temperatures  $T_{\alpha, 1\text{Hz}}^{\text{DMA}}$  are more or less comparable to the glass temperatures  $T_g$  as obtained by a midpoint construction from DSC heating scans performed with a rate of 20 K/min (Table 2).

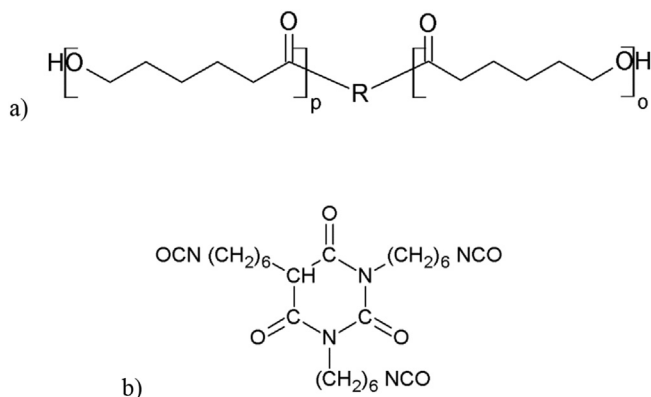
Certain differences seem to exist in particular for Capa™2085 and Capa™2125, but this is not unexpected since it is well known that the  $\alpha$  relaxation time at  $T_g$  is to a certain extent material dependent [39,40]. Accordingly, the temperature difference  $T_g - T_{\alpha, 1\text{Hz}}^{\text{DMA}}$  can vary depending on the material.

Note that there is a pronounced shoulder in the low temperature data indicating an additional relaxation process with a maximum between –100 °C and –90 °C. This evidences the existence of a secondary  $\beta$  relaxation process in this frequency-temperature range which is confirmed by dielectric spectroscopy as discussed below.

The storage part of the elastic modulus  $E'$  in the rubber plateau range shows a clear increase with decreasing average molecular weight  $M_w$  of the diol sequences. Values for the crosslink density  $\nu$  estimated based on simple rubber elasticity models and the rubber plateau modulus  $E_{N\sim E'}^0$  (35 °C) are given in Table 1. As expected  $\nu$  increases systematically with decreasing  $M_w$  since the molecular weights between neighbored crosslinks  $M_c$  is inversely proportional to  $\nu$ . Interestingly, the storage modulus  $E'$  at temperatures below the  $\alpha$  relaxation is slightly but systematically dependent on the chosen Capa™ type, i.e., the average length of the diol sequences. The  $E'$  values are higher for short diol sequences and high  $\alpha$  relaxation temperatures. The cold crystallization process in Capa™2205 based polyurethane around 1 °C is also visible in the dynamic-mechanical data. An increase in the storage modulus  $E'$  is seen between –20 °C and 0 °C related to the growth of a solid (crystalline) fraction in the rubbery polymer network. A maximum in  $E'$  ( $T, 1\text{ Hz}$ ) is observed near 0 °C corresponding to the findings in DSC heating scans before a decrease occurs in  $E'(T)$  at higher temperatures related to melting of the crystalline fraction. A representative example for the results of dielectric spectroscopy measurements on one of the fully amorphous polyurethane networks under investigation is shown in Fig. 3.

The loss part of the dielectric function  $\epsilon''$  is presented in a 3D plot depending on logarithm frequency and temperature. The  $\alpha$  relaxation peak with strongly non-linear temperature dependence of the peak maximum frequency is clearly visible at temperatures above –30 °C.

Considering the isotherms of  $\epsilon'$  and  $\epsilon''$  at temperatures between –40 °C and 100 °C (Fig. 4) one can see that the  $\alpha$  relaxation process is clearly visible as a step in the real part  $\epsilon'$  and pronounced peak in the imaginary part  $\epsilon''$ . Apart from this  $\alpha$  peak, pronounced conductivity-like contributions according to  $\epsilon'' \propto \sigma/(\epsilon_0 \omega)$  (with  $\sigma$  being the DC conductivity and  $\epsilon_0$  the permittivity of free space) are observed in  $\epsilon''$  at low frequencies if the temperature is higher



**Scheme 1.** (a)  $\epsilon$ -caprolactone based systems Capa™2000 and (b) Desmodur™3300 the main component is a trimer of HDI.

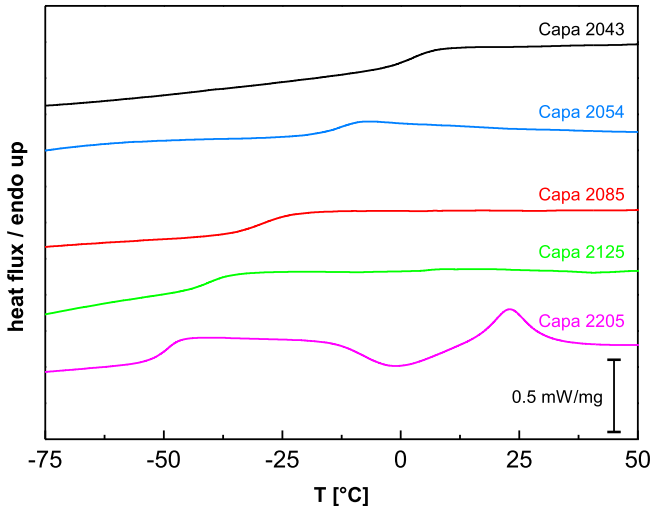


Fig. 1. DSC heating scans for five polyurethanes prepared based on Desmodur™3300 and different Capa™ systems.

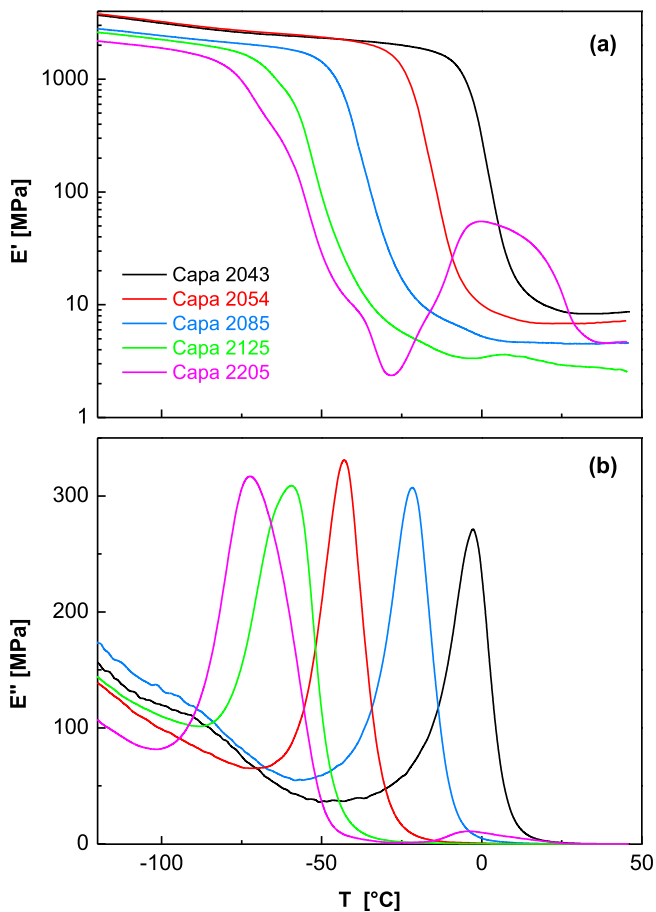


Fig. 2. (a) Storage modulus  $E'$  and (b) loss modulus  $E''$  as function of temperature for five polyurethanes made of Desmodur™N3300 and different Capa™ types.

than  $-30$  °C. In addition, much weaker secondary relaxation processes are detected at temperatures below  $-40$  °C down to  $-100$  °C (Fig. 5).

A broad bimodal peak in the loss part  $e''$  at the lowest temperatures indicates that there are indeed two superimposed secondary

relaxation processes ( $\beta$  and  $\gamma$ ).

In order to get deeper insights, a more detailed analysis of the dielectric isotherms has been performed based on fit of the experimental data to a sum of two or three Havriliak-Negami functions plus conductivity term

$$\varepsilon^*(\omega) = \varepsilon_\infty + \sum_k \frac{\Delta\varepsilon_k}{[1 + (i\omega/\omega_{0,k})^{b_k}]^{g_k}} = \varepsilon' - i\varepsilon'' \quad (1)$$

where  $\Delta\varepsilon_k$  and  $\omega_k$  are relaxation strength and characteristic frequency of the  $k^{\text{th}}$  relaxation process and  $b_k$  and  $g_k$  its shape parameters. The peak maximum frequency  $\omega_{max,k}$  characterizing the relaxation processes can be calculated based on

$$\omega_{max,k} = \omega_0 \left\{ \frac{\sin[\pi g_k b_k / (2g_k + 2)]}{\sin[\pi b / (2g_k + 2)]} \right\}^{-1/b_k} \quad (2)$$

Representative examples showing the quality of such fits are presented in Fig. 6.

The situation in  $\varepsilon''(\omega)$  isotherms at high temperatures with an  $\alpha$  relaxation peak as well as additional conductivity contributions at low frequencies and weak corrections due to secondary relaxations at high frequencies is shown in Fig. 6a. At lower temperatures, the  $\alpha$ ,  $\beta$  and  $\gamma$  relaxations partially overlap while conductivity contributions are negligible (Fig. 6b). Hence, the isotherms in this temperature range can be well described by three HN functions, where the  $\alpha$  process and  $\gamma$  process are most intense. Although it is relatively easy to determine the relaxation frequencies of the relaxation processes precisely, it is hard to get detailed information about shape parameters and relaxation strengths for all relaxation processes individually in those cases since they overlap significantly in the dielectric spectrum.

The temperature-dependent relaxation frequencies  $\omega_{max}$  for  $\alpha$ ,  $\beta$  and  $\gamma$  processes are plotted for all investigated polyurethanes in a common Arrhenius diagram (Fig. 7). Expectedly, the dynamic glass transition ( $\alpha$  relaxation) indicates a significantly non-linear dependence in the Arrhenius plot since the underlying segmental motions are cooperative.

This results in a strongly non-Arrhenius-like temperature dependence which can be approximated in a wide temperature range by the Vogel-Fulcher-Tamann-Hesse (VFTH) equation [41]

$$\log \omega_\alpha = \log \Omega_\alpha - B / (T - T_\infty) \quad (3)$$

with  $T_\infty$  being the Vogel temperature where the extrapolated  $\alpha$  relaxation time  $\tau_\alpha = 1/\omega_{\alpha,max} = 1/(2\pi f_{\alpha,max})$  would diverge,  $B$  is related to the curvature (roughly the higher  $B$  the lower curved is the  $\tau$  ( $1/T$ ) dependence), and  $\log \Omega_\alpha$  the limiting frequency for  $T \rightarrow 0$ . The VFTH fitting lines are shown in Fig. 7 and the corresponding parameters are listed in Table 2. The dielectric relaxation temperatures shift like in dynamic-mechanical data to lower values if the length of the diol component between the crosslinks increases. This trend and the observed  $\alpha$  relaxation temperatures themselves are also well line with the findings by DSC. Expectedly, the extrapolation to an  $\alpha$  relaxation time  $\tau_\alpha = 100$  s (corresponding to  $\omega = 2\pi f = 1/100$  rad/s) gives  $T_{\alpha,100s}^{DRS}$  values which are in approximate agreement with glass temperatures  $T_g$  from DSC heating scans with a rate of  $+20$  K/min. The observed  $T_g$  values are commonly about 10 K higher than  $T_{\alpha,100s}^{DRS}$ . To certain extent this is due to a relatively high heating rate ( $+20$  K/min). Otherwise, it is well known that the 100 s rule is only an approximation and that  $\tau_\alpha$  at  $T_g$  can vary for different materials at least between 10 and 1000 s [39,40].

Table 1 also includes the fragility parameter,  $m$  [42], that gives a measure of the departure from Arrhenius behavior quantified by the slope of the  $\alpha$  trace in the Arrhenius plot taken at  $T_g$  which can

**Table 2**  
Softening temperatures, activation energies and VFTH fit parameters.

Capa™	$T_g$ °C	$T_{\alpha}^{DMA}$ 1/Hz °C	$T_{\alpha}^{DRS}$ 100s °C	$E_{A,\beta}$ kJ/mol	$\log\Omega_{\beta}$ rad/s	$E_{A,\gamma}$ kJ/mol	$\log\Omega_{\gamma}$ rad/s	$T_{\infty}$ K	$B$ K	$\log\Omega_{\alpha}$ rad/s	$m$
2043	-3.1	-1.9	-10.7	62	17.9	45	17.1	219	610	12.1	84.9
2054	-13.5	-19.3	-23.6	45	12.6	45	17.3	210	553	12.0	89.0
2085	-32.5	-45.7	-42.3	59	17.4	36	14.9	187	635	12.5	76.2
2125	-39.9	-60.9	-51.1	63	18.8	41	16.5	186	476	11.4	83.1

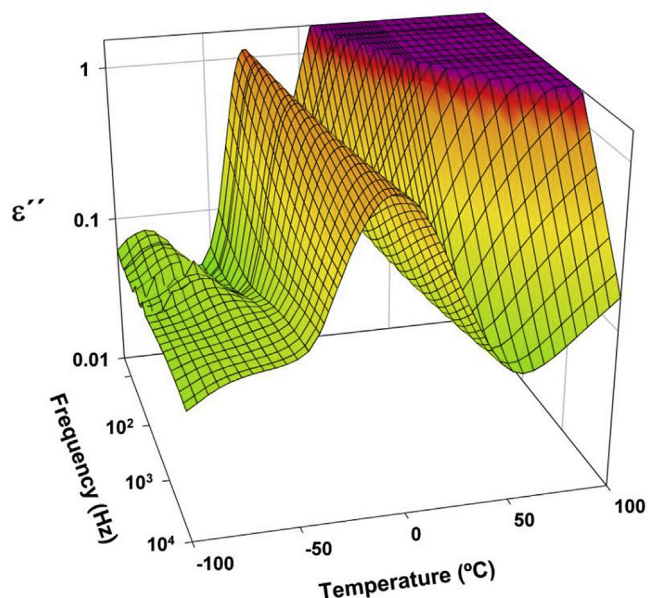


**Fig. 3.** Frequency-temperature dependence of the imaginary part of dielectric function for the polyurethane network prepared based on Desmodur™N3300 and Capa™2085.

be calculated based on the VFTH parameters [43].

$$m = \frac{BT_g}{(T_g - T_0)^2} \quad (4)$$

The thus calculated fragility parameters are comparable for all investigated polymers and allow classifying these materials as moderately fragile. This means that they undergo identical changes in their physical properties as approaching  $T_g$ . This behavior differs from the one exhibited by highly fragile materials whose temperature dependence varies abruptly close to the glass transition temperature. While the latter behavior is often reported for polymers with rigid or sterically hindered backbones and/or bulky side groups, less fragile polymers often have flexible chains allowing a more efficient packing during vitrification [43]. Although several exceptions are known [44], the here studied materials seem to obey this trend most probably due to the flexibility imprinted by the diol spacers.

Activation energies  $E_A$  and limiting frequencies  $\log\Omega$  of  $\beta$  and  $\gamma$  processes are also determined. The obtained values for both processes are listed in Table 2. The corresponding fitting lines are given in Fig. 7. The  $E_A$  values of the  $\gamma$  processes are quite similar ( $\approx 41 \pm 5$  kJ/mol) for all investigated polyurethane samples and the extrapolation to infinite temperatures gives values close to  $10^{14}$  Hz being the upper frequency limit for relaxational motions. The behavior of the  $\beta$  process is similar although the activation energies  $E_A$  and the  $\log\Omega$  values scatter significantly more. In general, the activation energies  $E_{A,\beta}$  ( $57 \pm 12$  kJ/mol) are significantly higher

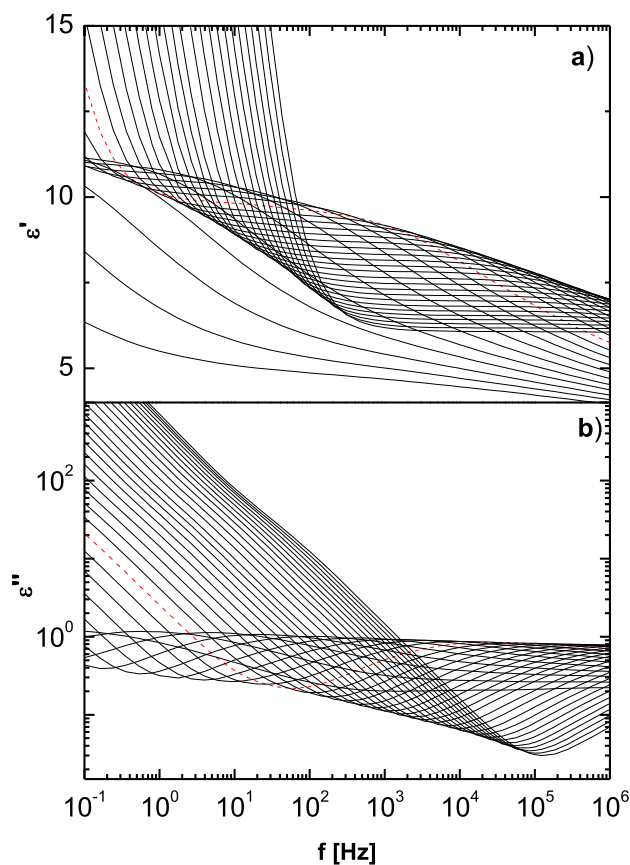


**Fig. 4.** (a) Real part  $\epsilon'$  and (b) imaginary part  $\epsilon''$  of the dielectric function as function of logarithm frequency for the polyurethane network prepared based on Desmodur™N3300 and Capa™2085 (mole ratio of the functional groups 1:1). The isotherms are measured at temperatures between 40 °C and 100 °C in steps of 5 K and at temperatures between -40 °C and 40 °C in steps of 4 K. The isotherm for 0 °C is shown as dashed line.

than those for the  $\gamma$  process. The larger scatter is possibly due to the fact that (I) the  $\beta$  intensity is commonly smaller than that of the overlapping  $\gamma$  relaxation and that (II) the  $\beta$  relaxation frequency is approaching that of the strong  $\alpha$  peak at higher temperatures. Hence, it is difficult to deconvolute the contributions from that of other relaxation processes and the uncertainties increase. In general, the relaxation processes,  $\beta$  and  $\gamma$ , show typical features of secondary relaxation processes in amorphous polymers related to fluctuative motions of small subunits on atomistic length scales. Such motions are only slightly influenced by changes of the overall packing of the molecules in their environment. This explains why these motions are practically unaffected below  $T_g$  despite of significant changes regarding the cooperative  $\alpha$  dynamics in the investigated series of polyurethanes. Similar behavior has been

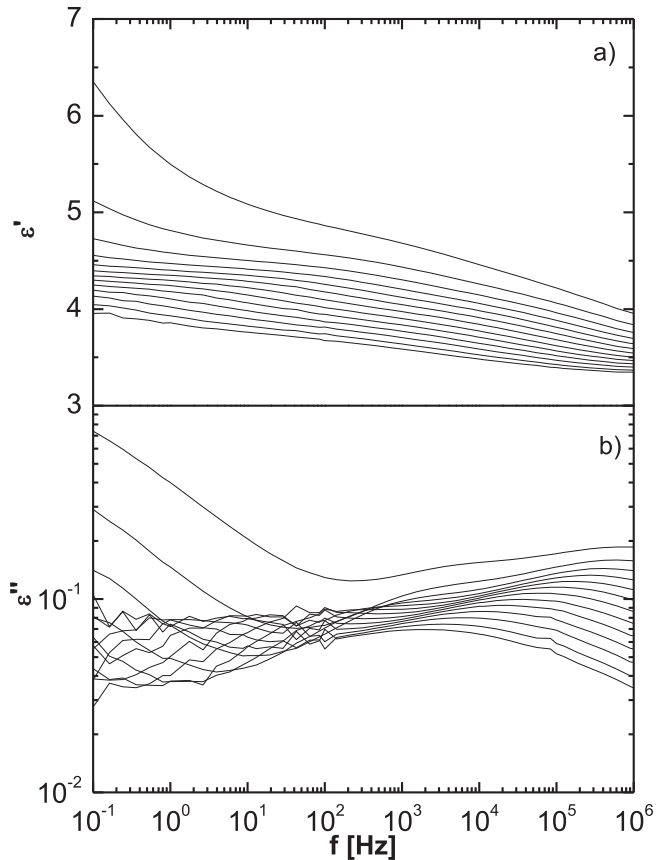


**Fig. 5.** (a) Real part  $\epsilon'$  and (b) imaginary part  $\epsilon''$  of the dielectric function versus logarithm frequency for the polyurethane network prepared based on Desmodur™N3300 and Capa™2085 (mole ratio of the functional groups 1:1) measured at temperatures between  $-100$  °C and  $-40$  °C in steps of 5 K.

observed for other amorphous polymer series where the glass transition temperature changes significantly due to internal plasticization by longer methylene sequences like poly (*n*-alkyl methacrylates) or poly (*n*-alkyl acrylates) [36,45,46].

Based on the existing information it seems to be interesting to check whether or not the  $\beta$  relaxations in polyurethanes studied here fulfill the criteria considered to be characteristic for Johari-Goldstein (JG) processes [47,48]. In particular, it is checked whether or not the estimated activation energy values  $E_{A,\beta}$  are compatible with the criterion for JG processes proposed by Kudlik et al. [49] according to which the ratio  $E_{A,\beta}/RT_{\alpha 100s}^{DRS}$  should be  $\sim 24$  ( $R$  is the universal gas constant). The obtained ratios are 28, 22, 31 and 34 for Capa™ 2043, 2054, 2085 and 2125, respectively. These values seem to be in the average compatible with the predictions by Kudlik et al. although a certain scatter around the expected value of  $\sim 24$  is clearly visible. Similar deviations have been reported earlier in several other cases indicating that it is not the  $E_{A,\beta}/RT_{\alpha 100s}^{DRS}$  value but the coupling between JG relaxation and cooperative  $\alpha$  relaxation that is most relevant [50]. Note that the values for the more intense  $\gamma$  relaxation in the investigated polyurethanes clearly differ from that what has been predicted for JG processes [49,50]. The activation energies obtained for the  $\gamma$  relaxations are relatively similar to those obtained for caprolactone and poly ( $\epsilon$ -caprolactones) [51].

Another interesting question that has been extensively studied in glass-forming polymers where  $\alpha$  relaxation times approach to those of a JG-like process in the so called  $\alpha\beta$  splitting region or  $\alpha\beta$  crossover region [45,52] is whether or not this feature is

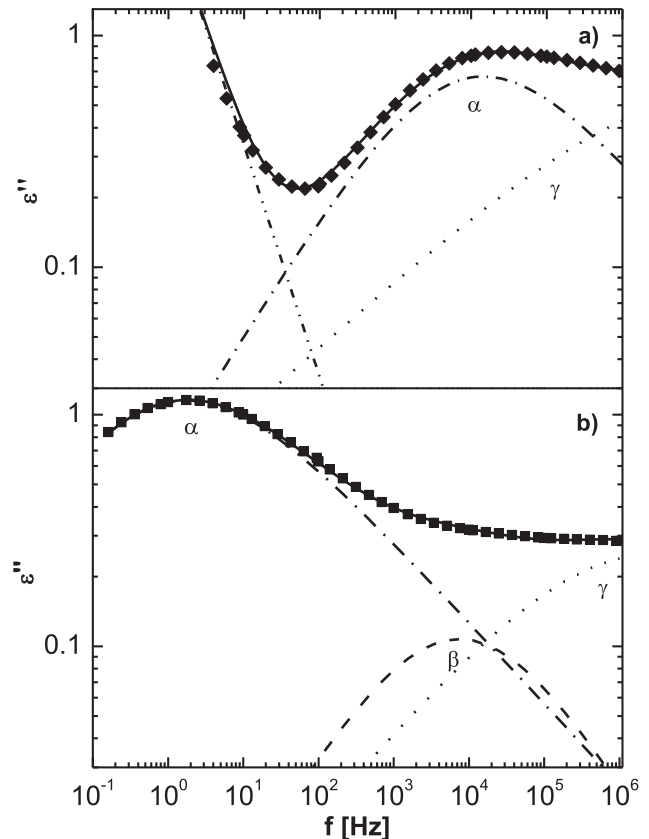


**Fig. 6.** Frequency dependence of the imaginary part  $\epsilon''$  of the dielectric function for polyurethane networks prepared based on Desmodur™N3300 and Capa™2085 at temperatures of (a)  $0$  °C and (b)  $-30$  °C (solid line - sum of all contributions, dashed and dotted lines - relaxation peaks, dashed double-dotted line - DC conductivity). The relevant relaxation processes ( $\alpha$ ,  $\beta$ ,  $\gamma$ ) are labeled in both parts.

accompanied by additional peculiarities in the relaxation dynamics. It has been demonstrated [53] for various polymeric and non-polymeric glasses that the  $\alpha\beta$  crossover is in many cases accompanied by (i) an intensity onset of the  $\alpha$  relaxation process, (ii) changes in the temperature dependence of the  $\alpha$  relaxation time and (iii) deviations from the Stokes-Einstein law regarding the diffusion behavior. Dielectric measurements of different polymers have shown that an extrapolation of  $\Delta\epsilon_\alpha$  vs. reciprocal temperature approaches 0 in the  $\alpha\beta$  crossover region where  $\alpha$  and  $\beta$  relaxation times become comparable [52,53].

A more detailed inspection of the temperature-dependent dielectric  $\alpha$  relaxation strengths for the investigated polyurethanes underlines that the intensity  $\Delta\epsilon_\alpha$  is also in our samples systematically decreasing with increasing temperature. Fig. 8 further demonstrates that  $\Delta\epsilon_\alpha$  is roughly proportional to  $1/T$  as reported in other cases [45,46]. A linear extrapolation of the normalized  $\Delta\epsilon_\alpha$  values as function of  $1/T$  gives onset temperatures  $T_{on}$  of  $107.5$  °C,  $91.3$  °C,  $54.5$  °C, and  $56.2$  °C for Capa™ 2043, 2054, 2085 and 2125, respectively. These values are obviously in reasonable agreement with  $\alpha\beta$  crossover temperatures  $T_{\alpha\beta}$  defined as temperature where frequency gap between the (extrapolated)  $\alpha$  and  $\beta$  traces in the Arrhenius plot (Fig. 8) reach a minimum. Using the Activation energies, pre-factors and VFTH parameters given in Table 2 one gets  $112.2$  °C,  $70.1$  °C and  $65.2$  °C for Capa™ 2043, 2085 and 2125, respectively. A serious analysis for Capa™ 2054 was impossible since the number of data points for the  $\beta$  relaxation process is very

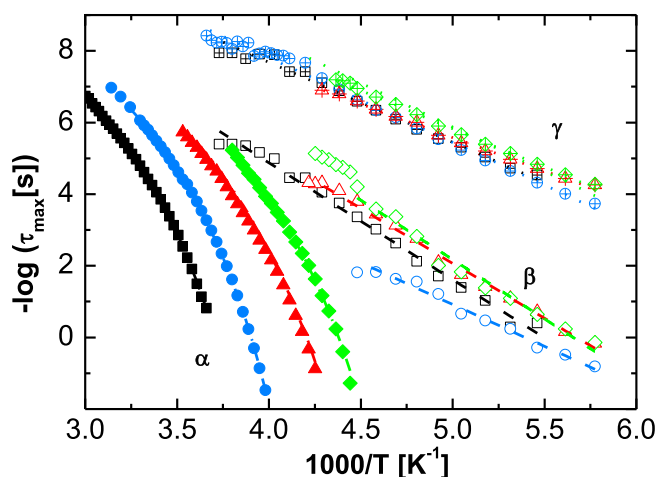


**Fig. 7.** Arrhenius plot showing the dielectric relaxation times for different relaxation processes in polyurethane networks composed of Desmodur™N3300 and Capa™2043 (squares), Capa™2054 (circles), Capa™2085 (triangles) and Capa™2125 (diamonds). Data for the  $\alpha$  relaxation (full symbols),  $\beta$  relaxation (open symbols), and  $\gamma$  relaxation (cross at center) are compiled.

limited leading to extremely large uncertainties regarding activation energy and intercept. Note that the temperature where  $\alpha$  and  $\gamma$  relaxation times approach each other ( $T_{\alpha\gamma}$ ) are significantly higher than  $T_{on}$  indicating that the interrelation between  $\alpha$  and  $\beta$  relaxations probably is most important.

Despite of remaining uncertainties one can conclude that there is for polyurethane networks evidence for an onset of the cooperative  $\alpha$  dynamics in the  $\alpha\beta$  crossover region. This confirms a central finding reported in the related literature and underlines the importance of the  $\alpha\beta$  crossover region for a deeper understanding of the cooperative  $\alpha$  motions. Obviously, the dielectric results reported here support the idea that cooperativity comes to an end at a finite temperature  $T_{on}$  in the  $\alpha\beta$  crossover region. It has been argued [52,54] that cooperativity might not be required any longer at  $T > T_{on}$  due to increasing free volume in the sample. Hence, the system becomes at high temperatures dynamically more homogeneous and an important prerequisite for the localized  $\beta$  motions has disappeared. Accordingly, the dynamics that survives above the  $\alpha\beta$  crossover region is qualitatively different from that what is appearing at temperatures  $T < T_{on}$ . Following this physical picture developed based on results for other polymers in the literature [51–53] the high temperature process  $a$  above  $T_{\alpha\beta} \approx T_{on}$  is neither a simple continuation of the  $\alpha$  process nor of the  $\beta$  process but a qualitatively different relaxation process.

#### 4. Conclusions

Summarizing the results of relaxation studies on a series of polyurethane networks one can conclude that the segmental  $\alpha$  dynamics of these systems depends systematically on the diol units between neighbored crosslinks.  $T_g$  and the softening temperatures from dynamic-mechanical data ( $T_{\alpha}^{DMA}$ ) and dielectric relaxation spectroscopy ( $T_{\alpha}^{DRS}$ ) decrease if the length of the diol spacers increase. More specifically it can be shown that this effect is due to an increasing number of methylene units  $n$  per diol spacer, or in other words an increasing fraction of  $\text{CH}_2$  units in the entire sample. Accordingly, we assume that internal plasticization effects should be responsible for this systematic dependence like in side-chain polymers with highly flexible alkyl groups of different lengths. This can be used to fine tune the properties of polyurethane networks made from diol units like Capa™ systems with different

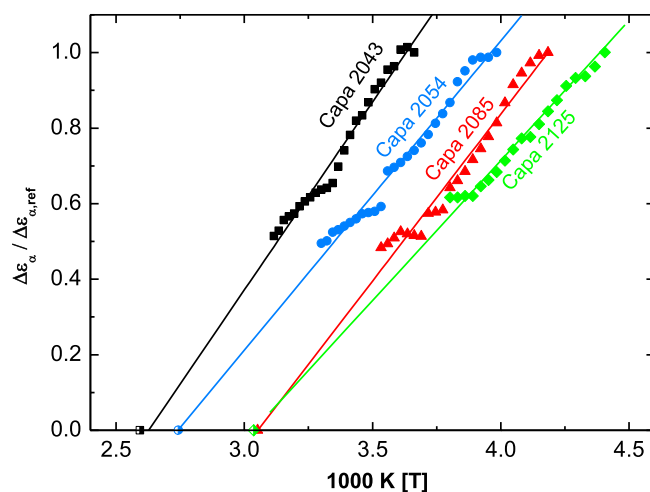


**Fig. 8.** Dependence of the normalized  $\alpha$  relaxation strength  $\Delta\epsilon_{\alpha}/\Delta\epsilon_{\alpha,ref}$  on reciprocal temperature  $1000/T$  for different polyurethane model networks composed of Desmodur™N3300 and Capa™2043 (squares), Capa™2054 (circles), Capa™2085 (triangles) and Capa™2125 (diamonds). The lines are linear fits aimed to estimate an onset temperature  $T_{on}$  by extrapolation. The half filled symbols correspond to the extrapolated  $T_{on}$  values. The  $\Delta\epsilon_{\alpha}$  values correspond to the maximum of  $\Delta\epsilon_{\alpha}$  in the investigated temperature interval.

molecular weight and isocyanate units like Desmodur™ acting as crosslinker.

Another interesting observation of this study is that a detailed analysis of the dielectric spectra clearly indicates an onset of the  $\alpha$  relaxation strength  $\Delta\epsilon_{\alpha}$  in the  $\alpha\beta$  crossover region of amorphous polyurethane model networks. Obviously,  $\Delta\epsilon_{\alpha}$  is roughly proportional to  $1/T$ . A linear extrapolation gives commonly onset temperatures  $T_{on}$  which are comparable with the crossover temperatures  $T_{\alpha\beta}$  where the difference between the relaxation times of  $\alpha$  relaxation and  $\beta$  relaxation shows a minimum. This observation is interpreted as an indication for an onset of the cooperative  $\alpha$  dynamics in the  $\alpha\beta$  crossover region and is well in line with the conclusions of earlier studies on other amorphous polymers and glasses. The fact that peculiarities regarding the  $\alpha$  intensity are only found in the  $\alpha\beta$  crossover region although two secondary relaxation processes,  $\beta$  and  $\gamma$ , exist in all investigated polyurethane networks underlines that there are in particular strong interrelations between the segmental  $\alpha$  dynamics and localized  $\beta$  motions in polyurethane networks. One can understand this experimental observation as additional support for the hypothesis that the dynamics of glass-forming materials changes in the  $\alpha\beta$  crossover region qualitatively. There is increasing evidence for the idea that the intermolecular cooperativity accompanied by dynamic heterogeneities disappears at temperatures above the  $\alpha\beta$  crossover temperature. To understand whether or not this is a general feature for various glass-forming materials seems to be of fundamental importance for a better understanding of the nature of cooperative  $\alpha$  motions and should be further studied in the future.

#### Acknowledgements

This work was sponsored by the Federal Ministry of Education and Research.

#### References

- [1] G. Oertel, *Polyurethane Handbook*, second ed., Hanser München, 1994.
- [2] P. Simon, M. Fratricova, P. Schwarzer, H. Wilde, Evaluation of the residual stability of polyurethane automotive coatings by DSC. Equivalence of Xenotest and desert weathering tests and the synergism of stabilizers, *J. Therm.*

- Analysis Calorim. 84 (2006) 679–692.
- [3] M. Ginic-Markovic, N. Choudhury, J.G. Matison, D.R.G. Williams, Characterization of polyurethane coatings using thermoanalytical techniques, *J. Therm. Analysis Calorim.* 59 (2000) 409–424.
- [4] M. Rahman, H. Kim, Effect of polyisocyanate hardener on waterborne polyurethane adhesive containing different amounts of ionic groups, *Macromol. Res.* 14 (2006) 634–639.
- [5] V.E. Musteata, D. Filip, S. Vlad, D. Macocinschi, Dielectric relaxation of polyurethane biocomposites, *Optoelectron. Adv. Mater. - Rapid Commun.* 4 (2010) 1187–1192.
- [6] D. Craig, S. Tamburic, Dielectric analysis of bioadhesive gel systems, *Eur. J. Pharm. Biopharm.* 44 (1997) 61–70.
- [7] S. Guelcher, A. Srinivasan, J. Dumas, J. Didier, S. McBride, J. Hollinger, Synthesis, mechanical properties, biocompatibility, and biodegradation of polyurethane networks from lysine polyisocyanates, *Biomaterials* 29 (2004) 1762–1775.
- [8] K. Raftopoulos, I. Zegkinoglou, A. Kanapitsas, S. Kriptou, I. Christakis, A. Vassilikou-Dova, P. Pissis, Y. Savelyev, Dielectric and hydration properties of segmental polyurethanes, *Mater. Res. Innov.* 8 (2004) 134–135.
- [9] A. Kanapitsas, P. Pissis, J. Gomez Ribelles, M. Monleon Pradas, E. Privalko, V. Privalko, Molecular mobility and hydration properties of segmented polyurethanes with varying structure of soft- and hard-chain segments, *Mol. Mobil. Hydradion Polyurethanes* 71 (1999) 1209–1221.
- [10] L. Apekis, P. Pissis, C. Christodoulides, G. Spathis, M. Niaounakis, E. Kontou, E. Schlosser, A. Schönhals, H. Goehring, Physical and chemical network effect in polyurethane elastomers, *Prog. Colloid & Polym. Sci.* 90 (1992) 144–150.
- [11] G. Spathis, M. Niaounakis, E. Kontou, L. Apekis, P. Pissis, C. Christodoulides, Morphological changes in segmented polyurethane elastomers by varying the NCO/OH ratio, *J. Appl. Polym. Sci.* 54 (1994) 831–842.
- [12] A. Havranek, M. Ilavsky, J. Nedbal, M. Böhm, W. v. Soden, B. Stoll, Viscoelastic behaviour of model polyurethane networks in the main transition zone, *Colloid & Polym. Sci.* 265 (1987) 8–18.
- [13] A. Zlatanic, Z. Petrovic, K. Dusek, Structure and properties of triolein-based polyurethane networks, *Biomacromolecules* 3 (2002) 1048–1056.
- [14] H. Ishihara, I. Kimura, K. Saito, H. Ono, Infrared studies on segmented polyurethane-urea elastomers, *J. Macromol. Sci. Part B* 10 (1974) 591–618.
- [15] R. Stepto, Theoretical and experimental studies of network formation and properties, *Polymer* 20 (1979) 1324–1326.
- [16] M. Ionescu, Chemistry and Technology of Polyols for Polyurethane, Rapa Technology Limited, Shawbury, 2005.
- [17] A. Rizo, G. Fytas, R. Ma, C. Wang, V. Abetz, G. Meyer, Local molecular motion in polyurethane-poly(methylmethacrylate) interpenetrating polymer networks, *Macromolecules* 26 (1993) 1869–1875.
- [18] A. Vatalis, C. Delides, G. Georgoussis, A. Kyritsis, O. Grigorieva, L. Sergeeva, A. Brovko, O. Zimich, V. Shtompel, E. Neagu, P. Pissis, Characterization of thermoplastic interpenetrating polymer networks by various thermal analysis techniques, *Thermochim. Acta* 371 (2001) 87–93.
- [19] A. Kanapitsas, P. Pissis, L. Karabanova, L. Sergeeva, L. Apekis, Broadband dielectric relaxation spectroscopy in interpenetrating polymer networks of polyurethane-copolymer of butyl methacrylate and dimethacrylate triethylene glycol, *Polym. Gels Netw.* 6 (1998) 83–102.
- [20] H. Shirasaka, Polyurethane urea elastomer having monodisperse poly(oxytetramethylene) as a soft segment with a uniform hard segment, *Macromolecules* 33 (2000) 2776–2778.
- [21] P. Pissis, A. Kanapitsas, Y. Savelyev, E. Akhranovich, E. Privalko, V. Privalko, Influence of chain extenders and chain end groups on properties of segmented polyurethanes, II, Dielectric study, *Polymer* 39 (1998) 3431–3435.
- [22] K. Dusek, M. Duskova-Smrckova, J. Fedderly, G. Lee, J. Lee, B. Hartmann, Polyurethane networks with controlled architecture of dangling chains, *Macromol. Chem. Phys.* 203 (2002) 1936–1948.
- [23] T. Nicolai, Dielectric relaxation of linear and cross-linked polyurethane, *Macromolecules* 34 (2001) 8995–9001.
- [24] L. Okrasa, M. Zigon, E. Zagar, P. Czech, G. Boiteux, Molecular dynamics of linear and hyperbranched polyurethanes and their blends, *J. Non-Cryst. Solids* 351 (2005) 2735–2758.
- [25] P. Pissis, A. Kyritsis, G. Georgoussis, V. Shilov, V. Shevchenko, Structure–property relationships in proton conductors based on polyurethanes, *Solid State Ionics* 136–137 (2000) 255–260.
- [26] D. Fragiadakis, S. Dou, R. Colby, J. Runt, Molecular Mobility, Ion Mobility, Mobile Ion, Concentration in poly(ethylene oxide)-based polyurethane ionomers, *Macromolecules* 41 (2008) 5723–5728.
- [27] V. Di Noto, M. Vittadello, K. Yoshida, S. Lavina, E. Negro, T. Furukawa, Broadband dielectric and conductivity spectroscopy of Li-ion conducting three-dimensional hybrid inorganic-organic networks as polymer electrolytes based on poly(ethylene glycol) 400, Zr and Al nodes, *Electrochim. Acta* 57 (2011) 192–200.
- [28] G. Polizos, A. Kyritsis, P. Pissis, V. Shilov, V. Shevchenko, Structure and molecular mobility studies in novel polyurethane ionomers based on poly(ethylene oxide), *Solid State Ionics* 136–137 (2000) 1139–1146.
- [29] M. Ilavsky, K. Dusek, The structure and elasticity of polyurethane networks: 1. Model networks of poly(oxypropylene) triols and diisocyanate, *Polymer* 24 (1983) 981–990.
- [30] S. Opera, V. Musteata, V. Potolinca, Molecular dynamics of linear and cross-linked polyester urethanes studied by dielectric spectroscopy, *J. Elastom. Plast.* 43 (2011) 559–576.
- [31] S. Opera, Synthesis and Properties of new polyurethane elastomers: influence of hard segment structure, *Polimery* 55 (2) (2010) 111–117.
- [32] Perstorp Holding AB Sweden, Capa™ One molecule. Millions of opportunities, 2017 (accessed 17.01.2017), [http://virtualpu.com/uploads/user\\_doc\\_attachment/0-2013-08-28%2011:00:26-CAPA\\_eng.pdf](http://virtualpu.com/uploads/user_doc_attachment/0-2013-08-28%2011:00:26-CAPA_eng.pdf).
- [33] B. Müller, U. Poth, Coating Compendien: Lackformulierung und Lackrezeptur, 2. überarbeitete Auflage Vincentz Hannover, 2005.
- [34] M. Beiner, K. Schröter, E. Hempel, S. Reissig, E. Donth, Multiple glass transition and nanophase separation in poly(n-alkyl methacrylate) homopolymers, *Macromolecules* 32 (1999) 6278–6282.
- [35] M. Beiner, Relaxation in poly(alkyl methacrylate)s: crossover region and nanophase separation, *Macromol. Rapid Commun.* 22 (2001) 869–895.
- [36] M. Beiner, H. Huth, Nanophase separation and hindered glass transition in side-chain polymers, *Nat. Mater.* 2 (2003) 595–599.
- [37] V. Arrighi, A. Triolo, I. McEwen, P. Holmes, R. Triolo, H. Amenitsch, Observation of local order in poly(di-n-alkyl itaconate)s, *Macromolecules* 33 (2000) 4989–4991.
- [38] J. Heijboer, Mechanical properties and molecular structure of organic polymers, in: J.A. Prins (Ed.), *Physics of Non-crystalline Solids*, North Holland, 1995, pp. 231–254.
- [39] C.A. Angell, Relaxation in liquids, polymers and plastics crystals – strong/fragile patterns and problems, *J. Non-Cryst. Solids* 131–133 (1991) 13–31.
- [40] C.T. Moynihan, Structural relaxation and the glass transition, in: J.F. Stebbins, P.F. McMillan, D.B. Dingwell (Eds.), *Structure, Dynamics and Properties of Silicate Melts*, Reviews in Mineralogy, Mineralogical Society of America, Washington, 1995, pp. 1–19.
- [41] H. Vogel, The law of the relation between the viscosity of liquids and the temperature, *Phys. Z.* 22 (1921) 645–646.
- [42] R. Böhmer, K.L. Ngai, C.A. Angell, D.J. Plazek, Nonexponential relaxations in strong and fragile glass formers, *J. Chem. Phys.* 99 (1993) 4201–4209.
- [43] K. Kunal, C.G. Robertson, S. Pawlus, S.F. Hahn, A.P. Sokolov, Role of chemical structure in fragility of polymers: a qualitative picture, *Macromolecules* 41 (2008) 7232–7238.
- [44] A.P. Sokolov, V.N. Novikov, Y.J. Ding, Why many polymers are so fragile, *J. Phys. Condens. Matter* 19 (2007) 205116, 8p.
- [45] F. Grawe, A. Schönhals, H. Lockwenz, M. Beiner, K. Schröter, E. Donth, Influence of cooperative alpha dynamics on local beta relaxation during the development of the dynamic glass transition in poly(n-alkyl methacrylate)s, *Macromolecules* 29 (1996) 247–253.
- [46] K. Schröter, R. Unger, S. Reissig, F. Garwe, S. Kahle, M. Beiner, E. Donth, Dielectric spectroscopy in the alpha beta splitting region of glass transition in poly(ethyl methacrylate) and poly(n-butyl methacrylate): different evaluation methods and experimental conditions, *Macromolecules* 31 (1998) 8966–8972.
- [47] G. Johari, M. Goldstein, Viscous liquids and the glass transition. II. Secondary relaxations in glasses of rigid molecules, *J. Chem. Phys.* 53 (1970) 2372–2388.
- [48] K. Ngai, M. Paluch, Classification of secondary relaxation in glass-formers based on dynamic properties, *J. Chem. Phys.* 120 (2004) 857–873.
- [49] A. Kudlik, C. Tschirwitz, T. Blochowicz, S. Benkhof, E. Rössler, Slow secondary relaxation in simple glass formers, *J. Non-Cryst. Solids* 235–237 (1998) 406–411.
- [50] K.L. Ngai, S. Capaccioli, Relation between the activation energy of the Johari-Goldstein  $\beta$  relaxation and  $T_g$  of glass formers, *Phys. Rev. E.* 69 (1–5) (2004) 031501.
- [51] M. Grimaud, E. Laredo, M.C. Pérez, Y.A. Bello, Study of dielectric relaxation modes in poly( $\epsilon$ -caprolactone): molecular weight, water sorption, and merging effects, *J. Chem. Phys.* 114 (2001) 6417–6425.
- [52] M. Beiner, S. Kahle, E. Hempel, K. Schröter, E. Donth, Two calorimetrically distinct parts of the dynamic glass transition, *Europhys. Lett.* 44 (1998) 321–327.
- [53] M. Beiner, H. Huth, K. Schröter, Crossover region of dynamic glass transition: general trends and individual aspects, *J. Non-Cryst. Solids* 279 (2001) 126–135.
- [54] E. Donth, H. Huth, M. Beiner, Characteristic length of the glass transition, *J. Phys. Condens. Matter* 13 (2001) L451–L462.